

Neural Networks for the Benchmarking of Detection Algorithms

Silvia Miramontes

mirasilva@lbl.gov

Lawrence Berkeley National Laboratory
University of California, Berkeley
Berkeley, California

Daniela Ushizima (advisor)

dushizima@lbl.gov

Lawrence Berkeley National Laboratory
University of California, Berkeley
Berkeley, California

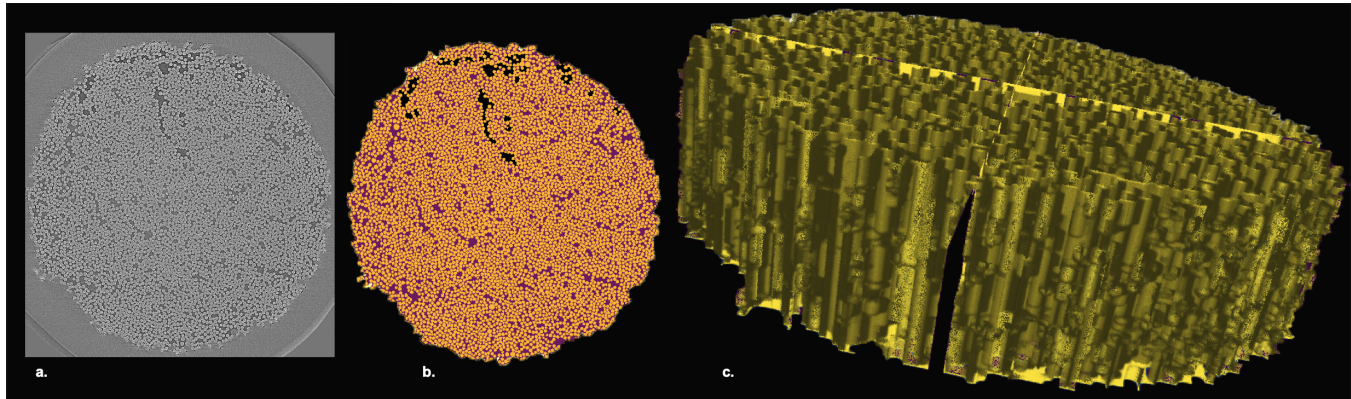


Figure 1: Evaluation of a fiber detection model: (a) raw data and (b) detected fibers in white from cross-section in the middle of stack; (c) rendering of detected fibers to emphasize discontinuities that are artifact from detection model.

ABSTRACT

There are several automated methods to detect objects from grayscale images. However, materials scientists still lack basic tools to compare different detection results, particularly when working with microtomography. This paper introduces FibCAM, a convolutional neural network (CNN)-based method using TensorFlow that allows benchmarking fiber detection algorithms. Our contribution is three-fold: (a) the design of a computational framework to compare automated fiber detection models with curated datasets through classification; (b) lossless data reduction by embedding prior knowledge into data-driven models; (c) a scheme to decompose computation into embarrassingly parallel processes for future analysis at scale. Our results show how FibCAM classifies different structures, and how it illustrates the material's composition and frequency distribution of microstructures for improved interpretability of machine learning models. The proposed algorithms support probing the specimen content from gigabyte-sized volumes and enable pinpointing inconsistencies between real structures known a priori and results derived from automated detections.

CCS CONCEPTS

- Computing methodologies → Artificial intelligence; Computer vision; 3D imaging; Object recognition;

KEYWORDS

Computer vision, Materials science, CNN

ACM Reference Format:

Silvia Miramontes and Daniela Ushizima (advisor). 2019. Neural Networks for the Benchmarking of Detection Algorithms. In *SC '19: ACM Student Research Competition Posters, Denver, CO*. ACM, New York, NY, USA, 4 pages. <https://doi.org/10.1145/1122445.1122456>

1 INTRODUCTION

Object detection algorithms often target specific image structures or corresponding polygons, aim to speed up the screening of large image datasets, and identify regions of interest before running more specialized algorithms. For example, a volume cross-section may contain fiber profiles, which are frequently correlated with the presence of elliptical shapes surrounded by high contrast coating. Counting and characterizing fibers are tasks particularly important on the research of ceramic matrix composites (CMCs) [2, 3]. CMCs have special properties for aviation manufacturing: it is a relatively light material that can withstand high temperatures and loads. Shape and structural properties of such compounds are imaged through X-rays, generating microtomography (microCT) images, used for materials quality control [1].

Scientific experiments to stress test CMCs can generate terabyte-sized datasets [7–9], which demand automated algorithms. Such

Permission to make digital or hard copies of all or part of this work for personal or classroom use is granted without fee provided that copies are not made or distributed for profit or commercial advantage and that copies bear this notice and the full citation on the first page. Copyrights for components of this work owned by others than ACM must be honored. Abstracting with credit is permitted. To copy otherwise, or republish, to post on servers or to redistribute to lists, requires prior specific permission and/or a fee. Request permissions from permissions@acm.org.

SC '19, November 19–21, 2019, Denver, CO

© 2019 Association for Computing Machinery.

ACM ISBN 978-1-4503-9999-9/18/06...\$15.00

<https://doi.org/10.1145/1122445.1122456>

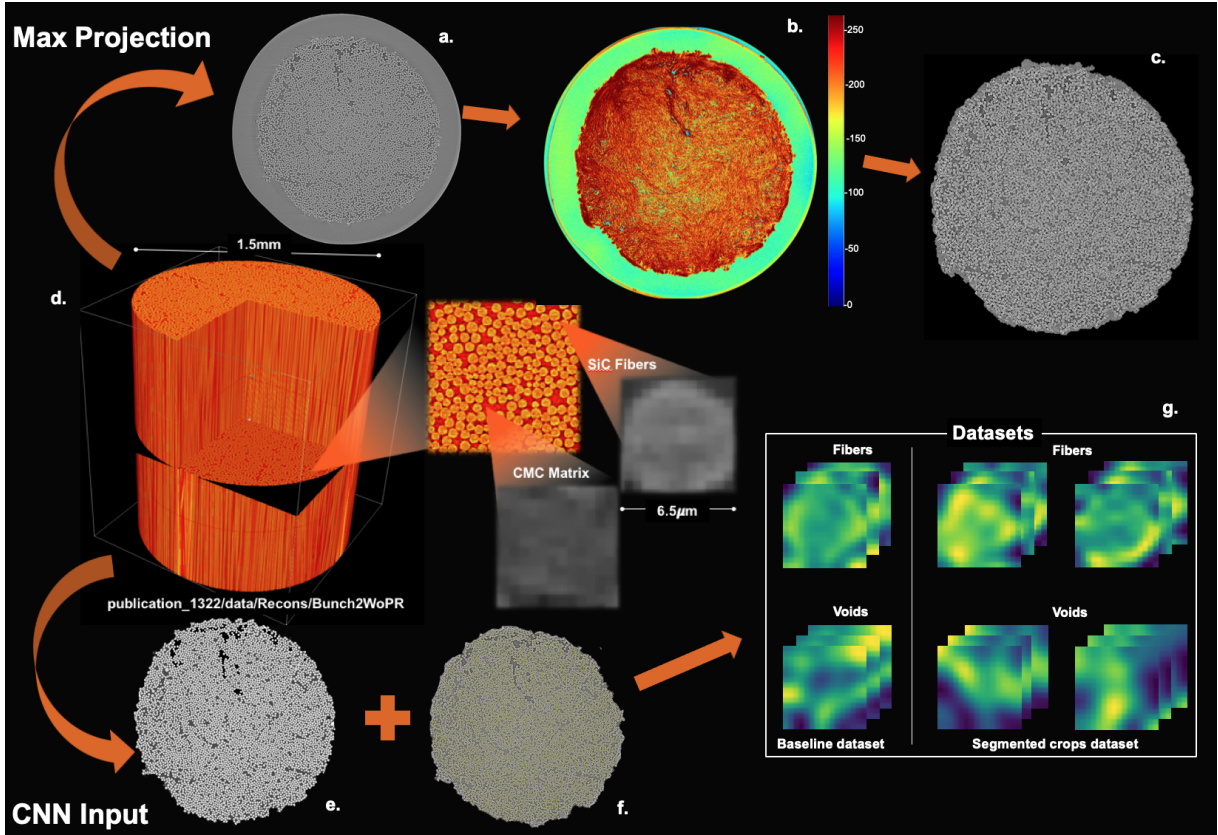


Figure 2: Multiscale image analysis: (a) Raw microCT image cross-section, (b) Maximum projection of volume over z-axis: red indicates high density of material, (c) Data reduction (65%) using mask based on maximum projection, (d) Global view of CMC specimen and local analysis of fibers, (e) Segmentation result by [6], (f) Manual labeling by human expert, (g) Creation of labeled datasets: the baseline and crops generated from results in [6] for entire stack.

demand has been met with numerous models for finding “fiber profiles” within microCT cross-sections, also known as fiber detection algorithms [4, 6, 11]. One major challenge is to compare these different detection approaches quantitatively, including 3D information. Fig. 1 shows an example in which fiber detection results look appropriate when observed in 2D, however false fiber discontinuities permeate the whole result as shown in the 3D rendering. Another challenge is to process microCT with billions of voxels for discovery of new material configurations, and to achieve autonomous experimentation in many steps of the scientific process.

2 MATERIALS

The X-ray microtomography images acquired in the investigation of the microstructure evolution during the matrix impregnation and curing in unidirectional fiber beds are publicly available at the Materials Facility website [9]. These are also fully described in Larson et al [6].

FibCAM experiments used thousands of cross-sections from a single fiber-reinforced CMC specimen, specifically two modes: the “raw image stack” and the “ground-truth stack”. The first set contains 2,160 image cross-sections from raw microCT data, while the second stack contains 1,000 image cross-sections of the segmented

results by [6], as [6] only includes the segmentation results for image slices (159-1158). We ensure that in our experiments the image slices from the raw stack correspond to the same slices as those in the segmented stack.

3 METHODS

3.1 Specimen Analysis with CNN

In order to properly access inaccurate detections, FibCAM uses manual labeling of a human expert as part of the training and classification of images. Expertise includes the ability to identify the composition of CMC phases and placement of fibers within a specimen. We create two datasets containing image crops of fibers and void spaces via scikit-image [12] (also known as fiber bed Fig. 2). The *baseline dataset* is derived from the work of a human expert, containing 8,814 images.

The *segmented crops dataset* is composed of 9,195,819 image crops generated following the results of the fiber model in [9], which may or may not contain inaccurate detections. To successfully compare the expert’s manual labeling with the *segmented crops dataset*, we train our LeNet-5 [10] based CNN with the *baseline dataset*, targeting a binary classification problem (“fiber” vs “non-fiber”). With a 70% - 30% train-test split we obtain an accuracy

Table 1: Classification results and augmentation by rotation of the segmented crops dataset.

Crops	Accuracy	Precision	Specificity	Sensitivity
Segmented	0.9161 ± 0.0041	0.9726 ± 0.0055	0.9568 ± 0.0082	0.8922 ± 0.0051
Augmented	0.9319 ± 0.0059	0.9429 ± 0.0088	0.9015 ± 0.0145	0.9496 ± 0.0033

of 95.99% and a test loss of 0.1110, which is illustrated in Fig. 3. Henceforth, we proceed to classify a subset of the segmented crops dataset, and its augmentation achieved by the rotation of each image at 90°.

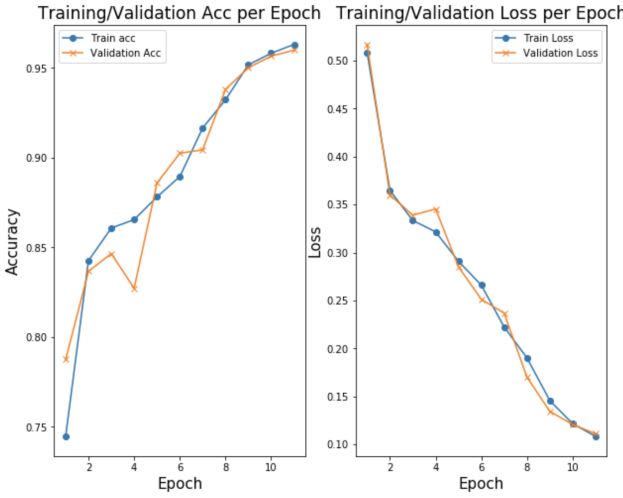


Figure 3: LeNet Performance for the training and validation of the baseline dataset with matplotlib package [5].

Moreover, FibCAM also contains python codes that automatically account for the number of fibers and fiber area per slice for the entire stack. FibCAM's quantitative analysis emphasizes the large variation of fiber cross sectional area that goes beyond the expected fiber diameters specified by the manufacturer (13-20 pixels). Also notice the fiber count oscillations across the stack, which indicate inaccuracies in the segmentation model [9] since no fiber breaks were expected in that CMC sample.

4 RESULTS AND CONCLUSION

The classification performance of the CNN model in Table 1 in terms of the sensitivity and specificity rates indicate that the fiber detection model presented in [6] hardly mislabeled non-fibers as fibers, but still missed a few true fibers. FibCAM experiments presented 2 main issues: a relatively small training set and limited generalization to the variety of fiber profiles.

Future work will address training size and variability to improve the accuracy of our CNN-based benchmarking system during evaluation of fiber detection methods, including support to eliminate false negatives from the results of such models. Because of the parallel nature of the CNN fiber-profile prediction algorithm, chunks

of the original microCT volume can be processed separately in different computing cores with minimum communication. In doing so, we expect to take advantage of multi-core/many-core architectures available at DOE scientific computing facilities. Further efforts will explore parallelization using libraries such as joblib and dask.

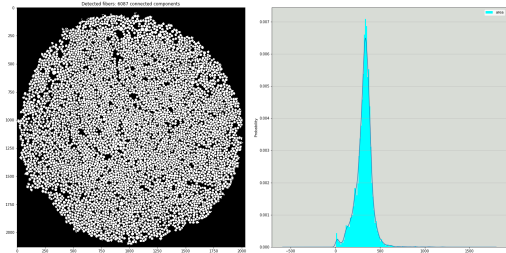


Figure 4: Fiber segmentation (left) and fiber area counts for slice #640 (right), also in Fig. 2(e).

ACKNOWLEDGMENTS

This research is supported by the Office of Science of the US Department of Energy under Contract No. DE-AC02-05CH11231 with Center of Advanced Mathematics for Energy Research Applications (CAMERA), the Gordon and Betty Moore Foundation through Grant GBMF3834, and the Alfred P. Sloan Foundation through Grant 2013-10-27 to the University of California, Berkeley.

REFERENCES

- [1] Araujo, Silva, Medeiros, Parkinson, Hexemer, Carneiro, and Ushizima. 2018. Reverse image search for scientific data within and beyond the visible spectrum. *Expert Systems with Applications* 109 (Nov 2018), 35–48.
- [2] Hirishkesh A Bale, Abdel Haboub, Alastair A Macdowell, James R Nasiatka, Dilworth Y Parkinson, Brian N Cox, David B Marshall, and Robert O Ritchie. 2012. Real-time quantitative imaging of failure events in materials under load at temperatures above 1,600 C. *Nat. Mater.* 12 (2012), 40–46.
- [3] B. N. Cox, H. A. Bale, M. Blacklock, M. Novak T. Fast, V. Rajan, R. Rinaldi, R. O. Ritchie, M. Rossol, J. Shaw, Q. D. Yang, F. Zok, and D. B. Marshall. 2014. Stochastic Virtual Test Systems for Ceramic Matrix Composites. *Annual Review of Materials Research* 44 (2014), 479–529.
- [4] Monica J. Emerson, Kristine M. Jespersen, Anders B. Dahl, Knut Conradsen, and Lars P. Mikkelsen. 2017. Individual fibre segmentation from 3D X-ray computed tomography for characterising the fibre orientation in unidirectional composite materials. *Composites Part A: Applied Science and Manufacturing* 97, C (2017), 83–92. <https://doi.org/10.1016/j.compositesa.2016.12.028>
- [5] J. D. Hunter. 2007. Matplotlib: A 2D graphics environment. *Computing in Science & Engineering* 9, 3 (2007), 90–95. <https://doi.org/10.1109/MCSE.2007.55>
- [6] Natalie Larson, Charlene Cuellar, and Frank Zok. 2019. X-ray computed tomography of microstructure evolution during matrix impregnation and curing in 2 unidirectional fiber beds. *Composites. Part A, Applied Science and Manufacturing* (2019), 243–259.
- [7] Natalie Larson and Frank Zok. 2018. In-situ 3D visualization of composite microstructure during polymer-to-ceramic conversion. *Acta Materialia* (2018), 579–589.
- [8] Natalie Larson and Frank Zok. 2018. Insights from in-situ X-ray computed tomography during axial impregnation of unidirectional fiber beds. *Composites Part A, Applied Science and Manufacturing*. Publishing Elsevier (2018), 124–134.

- [9] Natalie M. Larson and Frank W. Zok. 2019. Ex-situ XCT dataset for X-ray computed tomography of microstructure evolution during matrix impregnation and curing in unidirectional fiber beds. <http://dx.doi.org/doi:10.18126/M2QM0Z>.
- [10] Bengio Y, Haffner Patrick, LeCun Y, Bottou L. 1998. Gradient-Based Learning Applied to Document Recognition. *Proc. IEEE* 86, 11 (1998), 2278–2324.
- [11] D. Ushizima, H. A. Bale, W. Bethel, P. Ercius, B. Helms, H. Krishnam, L. Grinberg, M. Haranczyk, M. A. A. Macdowell, K. Odziomek, D. Y. Parkinson, T. Perciano, R. Ritchie, and C. Yang. 2016. IDEAL: Images across Domains, Experiments, Algorithms and Learning. *Journal of Minerals, Metals and Materials* (2016).
- [12] Stefan Van der Walt, Johannes L Schönberger, Juan Nunez-Iglesias, François Boulogne, Joshua D Warner, Neil Yager, Emmanuelle Gouillart, and Tony Yu. 2014. scikit-image: image processing in Python. *PeerJ* 2 (2014), e453.